

Martensitic phase transformation in single crystal $\text{Co}_5\text{Ni}_2\text{Ga}_3$

Peng Chen · Ke Chen · Guang Heng Wu ·
Xi Xiang Zhang

Received: 19 October 2006 / Accepted: 25 March 2008 / Published online: 9 April 2008
© Springer Science+Business Media, LLC 2008

Abstract The magnetic, thermal, and transport properties of martensitic phase transformation in single crystal $\text{Co}_5\text{Ni}_2\text{Ga}_3$ have been investigated. The single crystal $\text{Co}_5\text{Ni}_2\text{Ga}_3$ shows martensitic transformation at 251 K on cooling and 254 K on warming. Large jumps in the temperature-dependent resistance curve, temperature-dependent magnetization curve, and temperature-dependent thermal conductivity curve are observed at martensitic transformation temperature (T_M). Negative magnetoresistance due to spin disorder scattering was observed in $\text{Co}_5\text{Ni}_2\text{Ga}_3$ single crystal at all temperature range. The temperature-dependent negative magnetoresistance shows a peak at T_M , which indicates that the spin disorder increases in the process of phase transition. $\text{Co}_5\text{Ni}_2\text{Ga}_3$ sample exhibits a temperature dependence of thermal conductivity $\kappa(T)$ ($d\kappa/dT > 0$) due to electrons being above temperature 100 K.

Introduction

Ferromagnetic shape memory alloys (FMSMAs) are drawing much attention due to their various technological applications and the prediction that the Heusler alloys should be half-metals [1]. It is well known that the half-metals are very important materials for spintronics. FMSMAs can undergo martensitic phase transformation from martensite phase to austenite phase by changing temperature or applying magnetic field [2–6]. Heusler alloy $\text{Co}_2\text{Ni}_{1-x}\text{Ga}_{1+x}$ with crystal structure B2 is a noticeable FMSMA, which resembles the fully investigated Ni_2MnGa in both their electron concentration and magnetic properties [7–13]. Compared with NiMnGa alloys, $\text{Co}_2\text{Ni}_{1-x}\text{Ga}_{1+x}$ has higher Curie temperature, better ductility, and better stability in preparation without the highly volatile element Mn. The strain and the magnetization of martensitic phase transformation in $\text{Co}_2\text{Ni}_{1-x}\text{Ga}_{1+x}$ have been investigated intensely. This paper reports the magnetic, electrical, and thermal properties of martensitic phase transformation in $\text{Co}_5\text{Ni}_2\text{Ga}_3$ single crystal.

P. Chen (✉)
Department of Physics, Southwest University,
Chongqing, China
e-mail: pchen@swu.edu.cn

K. Chen
Chongqing Electric Power College,
Chongqing, China

G. H. Wu
Beijing National Laboratory for Condensed Matter,
Institute of Physics, CAS, Beijing 100080, China

X. X. Zhang
Department of Physics, Hong Kong University of Science
and Technology, Kowloon, Hong Kong, China

Experiments and discussion

$\text{Co}_5\text{Ni}_2\text{Ga}_3$ single crystals were grown by the Czochralski method in a Crystalox MCGS-3 cold crucible system [14] using constituent elements (Co, Ni, and Ga) with a purity of 99.99%. The magnetic measurements were performed in a Quantum Design Superconducting Quantum Interference Device. The electrical transport properties were measured by the four-point technique with applied magnetic field perpendicular to the electrical current in a Quantum Design Physical Property Measurement System (PPMS-9). The thermal conductivity was measured using a longitudinal steady-state technique in PPMS.

Magnetic properties

Figure 1 shows the temperature dependences of magnetization measured upon warming and cooling in $\text{Co}_5\text{Ni}_2\text{Ga}_3$ single crystal under applied magnetic field 100 Oe. On cooling, the martensitic start transition temperature T_{RS} is 251 K and the martensitic finish transition temperature T_{RF} is 247 K. On warming, the reverse martensitic start transition temperature T_{MS} is 254 K and the reverse martensitic finish transition temperature T_{MF} is 263 K. A large temperature hysteresis is observed.

Temperature dependences of magnetization measured upon warming in $\text{Co}_5\text{Ni}_2\text{Ga}_3$ single crystal under different applied magnetic fields are presented in Fig. 2. The low-temperature martensite phase shows smaller magnetization than that of high-temperature austenite phase near martensitic

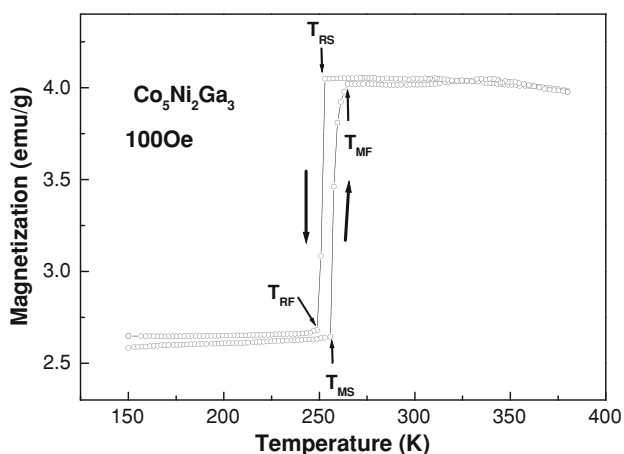


Fig. 1 Temperature dependence of magnetizations under magnetic field 100 Oe upon warming and cooling of $\text{Co}_5\text{Ni}_2\text{Ga}_3$ sample

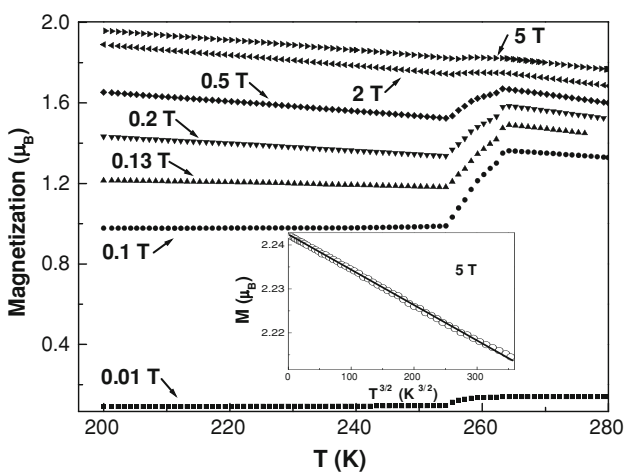


Fig. 2 Temperature dependences of magnetizations under various magnetic fields for $\text{Co}_5\text{Ni}_2\text{Ga}_3$ sample. The solid line in the inset graph is a linear fit to the $\text{Co}_5\text{Ni}_2\text{Ga}_3$ data, demonstrating the $T^{3/2}$ dependence of the magnetization for this low T range

transition temperature in all these applied magnetic fields. In relatively low field, this implies that martensite phase has a larger anisotropy. It is noticeable that, however, the low-temperature martensite phase shows smaller saturation magnetization than that of high-temperature austenite phase in applied magnetic field 50 kOe near martensitic transition temperature, which is different from $\text{Ni}_{5.19}\text{Mn}_{23.2}\text{Ga}_{24.9}$ where the low-temperature martensite phase shows bigger saturation magnetization than that of high temperature austenite phase [15]. In NiMnGa alloy, the magnetism is mainly from Mn atoms, while the moment of Ni is negligible. The large distance (about 4 Å) between the neighboring Mn atoms establishes the ferromagnetism in the alloy. Therefore, the variation of lattice parameters upon the martensitic transformation benefits the overall magnetization in the martensitic NiMnGa. On the other hand, the slightly lower saturating magnetization in martensite implies that the ferromagnetism is from a mutual contribution from both Co and Ni moments in CoNiGa system.

The temperature-dependent saturation magnetization behaves according to $M_S \sim T^{3/2}$ power law below temperature $T = 50$ K (Inset to Fig. 2), which indicates that the spin-wave excitation is allowed. Our measurement shows that the Curie temperature in $\text{Co}_5\text{Ni}_2\text{Ga}_3$ single crystal is above 400 K. Normally, the Heusler half-metal alloys predicted by theory show integer saturation magnetic moment [16–18]. The saturation magnetic moment at 2 K for $\text{Co}_5\text{Ni}_2\text{Ga}_3$ was extracted from the magnetization curve to be $2.242 \mu_B$ per f.u.

Electrical properties

The temperature dependence of resistance ρ measured upon warming and cooling of $\text{Co}_5\text{Ni}_2\text{Ga}_3$ single crystal is shown in Fig. 3. A large jump near temperature 250 K on

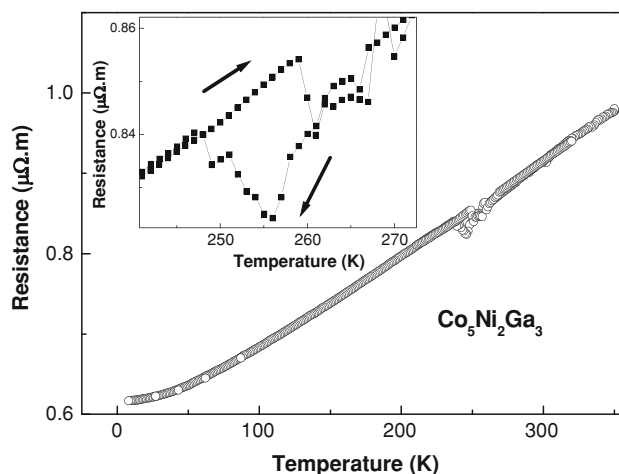


Fig. 3 Temperature dependence of resistivity upon warming and cooling for $\text{Co}_5\text{Ni}_2\text{Ga}_3$ sample. Inset shows the detail ρ - T curves upon warming and cooling near temperature 250 K for $\text{Co}_5\text{Ni}_2\text{Ga}_3$

cooling corresponds well to the martensitic transition observed magnetically (Inset to Fig. 3). The jump of ρ - T curve near 250 K on cooling is due to the scattering associated with the presentation of crystallographically equivalent variants in the martensite phase. The variants cause defects and twin boundaries due to the lattice deformation, which may increase the resistivity. On warming, the jump takes place at temperature 260 K (Inset to Fig. 3), which corresponds to the reverse martensitic transition temperature observed magnetically on warming.

The usual expression for the temperature dependence of resistivity for metals and alloys can be described by the Matthiessen rule $\rho(T) = \rho_0 + CT^n$. A plot of $\ln(\rho - \rho_0)$ as a function of $\ln(T)$ will yield the power-law parameter n (Fig. 4). For temperature $T < 70$ K, the resistivity behaves according to $\rho \sim T^{2.03}$ power law. It is known that, in the case of ferromagnetic elements such as Fe, Co, and Ni, the resistivity usually has a term proportional to T^2 at low temperature, which is ascribed to inelastic electron-phonon scattering from vibrating impurities. Above 70 K, the resistivity dependence transforms from $T^{2.03}$ dependence to an almost purely phononic linear dependence $n = 0.93$ in martensite phase and $n = 1.05$ in austenite phase.

Negative magnetoresistance ($MR = (\rho(H) - \rho(0))/\rho(0)$) was observed in $\text{Co}_5\text{Ni}_2\text{Ga}_3$ single crystal at all temperature range (Fig. 5). The resistivity decreases linearly with increasing magnetic field and does not saturate up to magnetic field 50 kOe (Inset to Fig. 5). The negative MR increases with temperature up to 320 K. The MRs were measured at various temperatures on warming. These characters indicate that the negative MR results from magnetic field suppression of the spin disorder scattering.

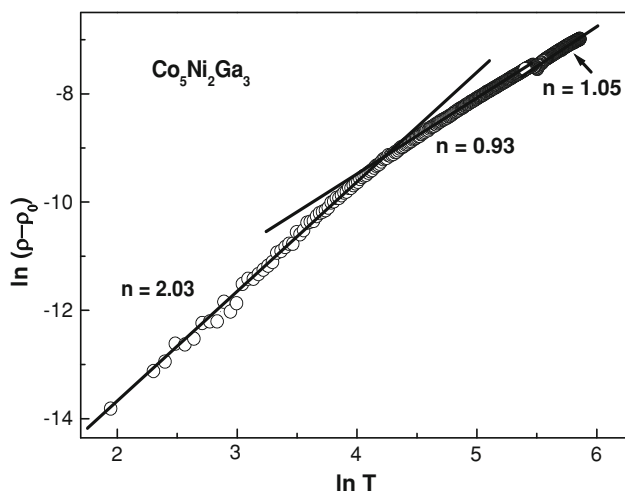


Fig. 4 $\ln(\rho - \rho_0)$ as a function of $\ln(T)$ for the $\text{Co}_5\text{Ni}_2\text{Ga}_3$ resistivity data. The slope of this curve corresponds to the power-law exponent n if we assume the functional form $\rho(T) = \rho_0 + cT^n$. The three distinct ranges of linearity are designated by lines, and labeled with the corresponding power-law exponent

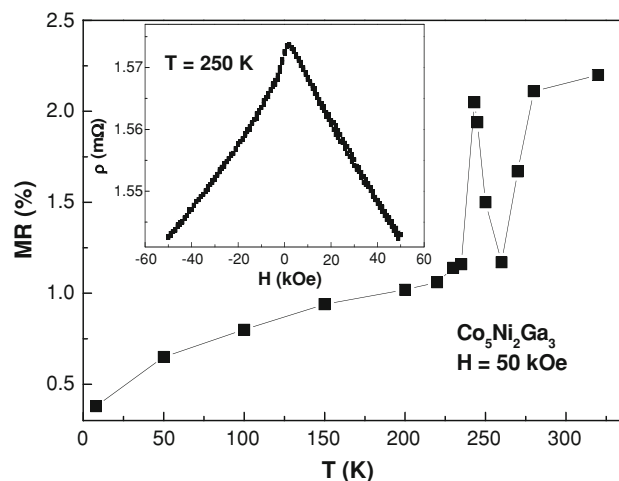


Fig. 5 Temperature dependence of magnetoresistance (MR) under magnetic field 50 kOe for $\text{Co}_5\text{Ni}_2\text{Ga}_3$ sample. Inset: The magnetic field-dependent resistivity at temperature 250 K

A jump was observed in MR - T curve at martensite-austenite transformation temperature, which indicates that the spin disorder in austenite phase is stronger than that in martensite phase. It is noticeable that a peak in MR - T curve appears near temperature 250 K, which indicates that the spin disorder increases in the process of phase transition.

Thermal properties

The temperature-dependent thermal conductivity, $\kappa(T)$, of the $\text{Co}_5\text{Ni}_2\text{Ga}_3$ single crystal sample on warming is shown in Fig. 6. Thermal conductivity of the $\text{Co}_5\text{Ni}_2\text{Ga}_3$ single crystal sample increases gradually from temperature

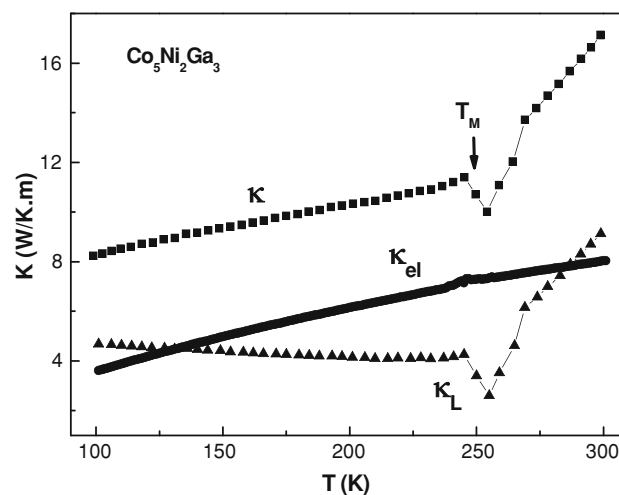


Fig. 6 The measured temperature-dependent thermal conductivity κ , the calculated electronic contribution to the thermal conductivity κ_{el} , and the contribution of the lattice to thermal conductivity $\kappa_L = \kappa - \kappa_{el}$ of the $\text{Co}_5\text{Ni}_2\text{Ga}_3$ sample

100–248 K, then decreases quickly from 248 to 258 K. It increases quickly above 258 K. The measured thermal conductivity (κ) should include the contribution of the lattice (κ_L) and the contribution of the electron (κ_{el}), that is to say $\kappa = \kappa_L + \kappa_{el}$. The electronic contribution to the thermal conductivity, κ_{el} , can be calculated using the Wiedemann–Franz law: $\kappa_{el} = L\sigma T$, where L is the Lorentz number, σ is the electrical conductivity, and T is the absolute temperature. The calculated temperature-dependent κ_{el} is shown in Fig. 6. κ_{el} increases with increasing temperature. The contribution of the lattice to thermal conductivity ($\kappa_L = \kappa - \kappa_{el}$) is shown in Fig. 6. Our results show that the measured thermal conductivity increases gradually with increasing temperature from 100 to 248 K, which should be attributed to electrons.

The character of $\kappa_L(T)$ curve shown in Fig. 6 accords with the kinetic expression for the contribution of the lattice to thermal conductivity, $\kappa_L = NCvl$, where N is the number of thermal carriers, C the specific heat, v the group velocity (usually assumed to be constant), and l the phonon mean free path. Above 100 K, the contribution of the lattice to thermal conductivity at high temperatures can be extrapolated using the Debye approximation [19], $l \sim 1/T$.

So κ_L decreases with increasing temperature from 100 to 248 K. On warming, the martensite–austenite transformation takes place at temperature 248 K and the lattice disorder increases. The phonon mean free path l decreases, and the contribution of the lattice to thermal conductivity κ_L decreases from 248 to 258 K. The martensite–austenite transformation nearly finishes at temperature 258 K and the order austenite forms. So the phonon mean free path l increases, and the contribution of the lattice to thermal conductivity κ_L increases above 258 K.

Summary

In summary, we have investigated magnetic, thermal, and transport properties of martensitic phase transformation in single crystal $\text{Co}_5\text{Ni}_2\text{Ga}_3$. Large jumps in the temperature-dependent resistance curve, temperature-dependent magnetization curve, and temperature-dependent thermal conductivity curve are observed at martensitic transformation temperature. Negative magnetoresistance due to spin disorder scattering was observed in $\text{Co}_5\text{Ni}_2\text{Ga}_3$ single crystal at all temperature range. $\text{Co}_5\text{Ni}_2\text{Ga}_3$ sample exhibits a temperature dependence of thermal conductivity $\kappa(T)$ ($d\kappa/dT > 0$) due to electrons being above temperature 100 K.

Acknowledgements In this paper was supported by a grant from the Science & Technology Commission, Chongqing, China (Project No. CSTC 2006BB2024 and SWNUF 2005002). XX Zhang would like to thank the support from HKUST grant 6059/02E.

References

- de Groot RA, Mueller FM, van Engen PG, Buschow KHJ (1983) Phys Rev Lett 50:2024. Ishida S, Masaki T, Fujii S, Asano S (1998) Physica B 245:1. Fujii S, Sugimura S, Ishida S, Asano S (1990) J Phys Condens Matter 2:8583. doi:10.1088/0953-8984/2/43/004
- Webster PJ, Ziebeck KRA, Town SL, Peak MS (1984) Philos Mag B 49:295. Fujita A, Fukamichi K, Gejima F, Kainuma R, Isshida K (2001) Appl Phys Lett 77:3054
- Furuya Y, Hagood NW, Kimura H, Watanabe T (1998) Mater Trans JIM 39:1248
- Wuttig M, Li J, Craciunescu C (2001) Scr Mater 44:2393. doi:10.1016/S1359-6462(01)00939-3
- Oikawa K, Wulff L, Iijima T, Gejima F, Ohmori T, Fujita A, Fukamichi K, Kainuma R, Isshida K (2001) Appl Phys Lett 79:3290. doi:10.1063/1.1418259
- Liu ZH, Zhang M, Cui YT, Zhou YQ, Wang WH, Wu GH, Zhang XX, Xiao G (2003) Appl Phys Lett 82:424. Liu ZH, Hu HN, Liu GD, Cui YT, Zhang M, Chen JL, Wu GH (2004) Phys Rev B 69:134415. doi:10.1103/PhysRevB.69.134415
- Chen F, Wang HB, Zheng YF, Cai W, Zhao LC (2005) J Mater Sci 40(1):219. doi:10.1007/s10853-005-5712-3
- Pirge G, Hyatt CV, Altintas S (2004) J Mater Sci Proc Tech 155–156:1266. doi:10.1016/j.jmatprotec.2004.04.225
- Meng FB, Li YX, Liu HY, Qu JP, Zhang M, Chen JL, Wu GH (2004) J Mater Sci Tech 20(6):697
- Li YX, Liu HY, Meng FB, Yan LQ, Liu GD, Dai XF, Zhang M, Liu ZH, Chen JL, Wu GH (2004) Appl Phys Lett 84(18):3594. doi:10.1063/1.1737481
- Sozinov A, Likhachev AA, Lanska N, Ullakko K (2002) Appl Phys Lett 80:1746. doi:10.1063/1.1458075
- Cherechukin AA, Dikshtein IE, Ermakov DI, Glebov AV, Koledov VV, Kosolapov DA, Shavrov VG, Tulaikova AA, Krasnoperov EP, Takagi T (2001) Phys Lett A 291:175. doi:10.1016/S0375-9601(01)00688-0
- Wang WH, Chen JL, Liu ZH, Zhan WS (2002) Appl Phys Lett 80:634. doi:10.1063/1.1447003
- Wu GH, Yu CH, Meng LQ, Chen JL, Yang FM, Qi SR, Zhan WS, Wang Z, Zheng YF, Zhao LC (1999) Appl Phys Lett 75:2990. doi:10.1063/1.125211
- Zhu FQ, Yang FY, Chien CL, Ritchie L, Xiao G, Wu GH (2005) J Magn Magn Mater 288:79. doi:10.1016/j.jmmm.2004.08.025
- Hordequin C, Ristoiu D, Ranno L (2000) Eur Phys J B 16(2):287. doi:10.1007/s100510070230
- de Groot RA, Mueller FM, van Engen PG, Buschow KHJ (1983) Phys Rev Lett 50:2024. doi:10.1103/PhysRevLett.50.2024
- Otto MJ, van Woerden RAM, van der Valk PJ (1989) J Phys Condens Matter 1:2341. doi:10.1088/0953-8984/1/13/007
- Oestreich J, Probst U, Rrichardt F, Bucher E (2003) J Phys Condens Matter 15:635. doi:10.1088/0953-8984/15/4/304